JOURNAL OF GUIDANCE, CONTROL, AND DYNAMICS
Vol. 22, No. 1, January–February 1999

Optimal Finite Thrust Orbit Transfers with Large Numbers of Burns

Troy Goodson* and Jason C. H. Chuang†
Georgia Institute of Technology, Atlanta, Georgia 30332
and
John Hanson‡
NASA Marshall Space Flight Center, Huntsville, Alabama 35812

This paper presents new theoretical results that are used to construct a new algorithm for the computation of fuel-optimal multiple-burn orbit transfers of low and medium thrust. Intuitively, one might want to think of an optimal multiple-burn transfer problem not as one large trajectory problem but as a sequence of optimal one-burn transfers between intermediate orbits that are optimally chosen. For spherical-body gravity, a strong relationship is shown to exist between these two problems. Theoretical results are used to transform the traditional set of necessary conditions to an equivalent set of conditions. Based on these results, a new numerical method that iteratively computes optimal orbit transfers is presented. Numerical results for an 11-burn transfer are presented to demonstrate the new algorithm.

Introduction

THE main objective of this research was the computation of fuel-optimal low- and medium-thrust orbit transfers. Here, medium thrust was taken as $1 > T/W_o \geq 0.01$ and low thrust as $0.01 > T/W_o \geq 0.001$, where T is the thrust level of the motor and W_0 is the weight of the spacecraft with respect to the gravitating body at the position and time just before the first burn. This particular definition has been made because it is the initial acceleration that the rocket motor produces compared with the gravitational acceleration at that point that determines how easily changes in the initial orbit will be made. In contrast, comparing the initial rocket motor acceleration with the gravitational acceleration as it would be measured on the planet's surface does not directly indicate the motor's ability to move the spacecraft away from a very high orbit.

Numerical methods for the computation of optimal orbit transfers have been widely studied. These numerical methods fall into three categories: direct, indirect, and hybrid methods.

Direct methods parameterize the thrust program and then attempt to optimize these parameters while satisfying boundary conditions. For example, Enright and Conway[1] demonstrated a successful scheme using collocation and nonlinear programming, in the vein of Hargraves and Paris[2]; additionally, a direct transcription approach was investigated by Enright and Conway[3] and furthered by Betts,[4] at least. Another interesting direct approach is differential inclusion, which has been investigated by Coverstone-Caroll and Williams[5] and Seywald.[6] Vulpetti and Montereali[7] used nonlinear programming to optimize medium-thrust transfers between inclined circular orbits with two–four burns.

Indirect methods employ the mathematics of optimal control to formulate a two-point boundary-value Problem (TPBVP), which can then be approached with a variety of numerical methods. Brown et al.[8] and Brown and Johnson[9] made use of a shooting method and some useful analytic simplifications to produce transfers with a few burns. Brusch and Vincent[10] also used a shooting method. McAdoo et al.[11] developed OPBURN, a combination of two indirect approaches. The first used a model for gravitational accelerations varying linearly with distance. The data from this approach were used as the starting iterate of another, more accurate code. Results with this method were presented for medium-thrust acceleration levels and two–three burns. Kluever and Pierson[12] used an indirect method, viz., shooting, to solve Earth–moon transfers using up to five burns; guesses were formed using a direct method. In that work, the moon's gravitational field came well into play; no such effects will be considered here. Redding[13] used an indirect method on noncoplanar circle-to-circle low Earth orbit–geosynchronous orbit problems; some results for a 16-burn solution and a 91-burn solution to that problem were presented. An exemplary theoretical development allowed Redding to predict certain characteristics of low-thrust transfers; such predictions were documented for transfers with up to 250 burns.

Hybrid methods are a combination of direct and indirect. These methods are often formed by simply removing difficult conditions from the TPBVP and optimizing some equivalent cost function over the unconstrained parameters. Ilgen[14] used a hybrid scheme called HYTOP to compute low-thrust transfers for an orbit transfer vehicle study. The HYTOP algorithm makes use of pointer vector continuity during a transfer. The pointer vector function, and only this function, was discretized into a piecewise linear function. The state was represented by equinoctial orbital elements. The final mass was then optimized over the choice of the pointer vector function parameters subject to the TPBVP constraints.

Zondervan et al.[15] used a hybrid method in a successful study of three-burn transfers with plane changes in ideal gravity and for thrust levels in the medium and low range. Their approach was to take the indirect setup and release the switching function constraint. The switching points were then optimized directly.

A common aphorism in this research area is that optimal transfers with large numbers of burns use less fuel than optimal transfers with small numbers of burns, when compared for the same set of terminal orbits and the transfer time is free.

The approach used by Redding[13] to obtain solutions with large numbers of burns requires that one solve the same optimization problem with fewer burns but an idential product of thrust × (number of burns). This approach then follows an algorithm reminiscent of homotopy whereby additional solutions are obtained, each successively with halved thrust and doubled number of burns. However, that method is based on varying only the initial conditions, as in shooting methods. Multiple shooting, which breaks a problem into several intervals and creates both additional equations and variables, is sometimes preferred over simple shooting. Perhaps an alternate approach could lead to improvements.

Received June 2, 1997; revision received June 22, 1998; accepted for publication July 1, 1998.

*Graduate Research Assistant, School of Aerospace Engineering; currently member of Technical Staff, Jet Propulsion Laboratory, California Institute of Technology, Pasadena, California 90119.

†Part-time Associate Professor, School of Aerospace Engineering; currently Senior Staff Engineer, Guidance, Navigation, and Control, Lockheed Martin Vought Systems, Grand Prairie, Texas 75051.

‡Chief, Flight Mechanics, Guidance, Navigation and Control Systems.

A new hybrid approach herein called the patched method has been developed. This method breaks the problem into two nested optimization problems: the fuel optimization of each thrusting arc as restricted by a fixed choice of coast arcs and the fuel optimization of that choice. The former problem is approached using either a direct method or an indirect method, viz., direct collocation or multiple shooting. The latter problem is approached with a conjugate-gradient method.

The bang-bang structure of the optimal orbit transfer solution means that the thrust is always either fully on or fully off. Optimal transfers are, therefore, made up of a series of individual interior transfers (thrusting arcs) between a sequence of orbits (coast arcs) beginning with the specified initial orbit and ending with the desired final orbit. However, the fact that these transfers are individually optimal transfers does not seem to be widely exploited yet. Later, this notion is expressed concisely in a mathematical sense and shown to be quite useful for numerical methods.

Orbit Transfer Modeling

The spacecraft is represented by a point mass and assumed to be a thrusting craft acted upon by spherical-body gravity forces of a central body. The central body, or planet, is also represented as a point mass positioned at its own center of gravity. Furthermore, the problem is restricted to crafts of mass much smaller than that of the central body; therefore, the planet is assumed fixed in inertial space. This inertial space is described with a rectangular Cartesian inertial reference frame (OXYZ). The central body is fixed at the center O of this frame and the z axis is perpendicular to that body's equator.

It is assumed that the fuel consumption rate of the motor is represented by

$$\dot{m} = -\frac{T}{g_o I_{sp}} \tag{1}$$

where m is the spacecraft's mass, T is the thrust, g_o is Earth's gravitational acceleration at sea level, and I_{sp} is the motor's specific impulse.

The equations of motion for the spacecraft are

$$\dot{\boldsymbol{x}}(t) = \boldsymbol{f}[\boldsymbol{x}(t), T(t), \boldsymbol{e}_T(t)] \tag{2}$$

where

$$\boldsymbol{x}(t) = [\boldsymbol{r}^T(t) \quad \boldsymbol{v}^T(t) \quad m(t)]^T \tag{3}$$

and

$$\boldsymbol{f}[\boldsymbol{x}(t), T(t), \boldsymbol{e}_T(t)] = \left\{ \begin{array}{c} \boldsymbol{v}(t) \\ \left[\dfrac{T(t)}{m(t)}\right]\boldsymbol{e}_T(t) - \dfrac{\mu \boldsymbol{r}(t)}{r^3(t)} \\ \dfrac{T(t)}{g_0 I_{sp}} \end{array} \right\} \tag{4}$$

where the position vector $\boldsymbol{r}(t) = [x(t) \;\; y(t) \;\; z(t)]^T$, the velocity vector $\boldsymbol{v}(t) = [u(t) \;\; v(t) \;\; w(t)]^T$, μ is the central body's gravitational parameter, and $\boldsymbol{e}_T(t)$ is the thrust direction vector. The thrust direction vector is constrained to have unity magnitude.

The thrust magnitude is constrained for all time $t \in [0, t_f]$:

$$0 \leq T \leq T_{max} \tag{5}$$

For problems in which the ideal, or spherical-body, gravity assumption is acceptable, coasting trajectories are well understood and can be analytically represented. Therefore, it is simplest to optimize the exit, or thrust on, point on the initial orbit and the entry, or thrust off, point on the final orbit. A real spacecraft implementing the orbit transfer could simply wait in the initial orbit until arrival at the initial orbit exit point, indicating that the maneuver should begin.

Hence, the boundary conditions must determine all orbital elements except position on orbit and are written as

$$\psi[\boldsymbol{x}(t_0)] = \alpha_0 \tag{6a}$$

$$\psi[\boldsymbol{x}(t_f)] = \alpha_f \tag{6b}$$

where the function ψ determines these orbital elements for the state in question and α_0 and α_f are vectors containing the desired values at the initial and final points, respectively. Obviously, the function is of one less dimension than its argument. Such a determination could be accomplished several different ways. However, using the angular momentum and eccentricity vectors is perhaps the simplest.[16] For planar transfers, all motion can be placed in the X–Y plane, and the components of the ψ function are

$$\psi_1 = h = xv - yu \tag{7a}$$

$$\psi_2 = \mu e_x = [(v^2 - \mu/r)x - (\boldsymbol{r}^T\boldsymbol{v})u] \tag{7b}$$

$$\psi_3 = \mu e_y = [(v^2 - \mu/r)y - (\boldsymbol{r}^T\boldsymbol{v})v] \tag{7c}$$

where h is the angular momentum, e_x is the X component of the eccentricity vector, and e_y is the Y component of the eccentricity vector.

In the three-dimensional case, these vectors have six components. Because the angular momentum and eccentricity vectors are always perpendicular, one of these components will be redundant and thus removable. There is one restriction on which component is removed—it can be seen clearly by considering the property that the vectors are always perpendicular, expressed as

$$h_x e_x + h_y e_y + h_z e_z = 0 \tag{8}$$

The six components are linearly dependent. A component of one of the two vectors can be removed if it can be computed using Eq. (8). If, for the orbit transfer problem in question, $h_z \neq 0$ on a terminal orbit, then the ψ function components can be written as the following:

$$\psi_1 = h_x = yw - zv \tag{9a}$$

$$\psi_2 = h_y = zu - xw \tag{9b}$$

$$\psi_3 = h_z = xv - yu \tag{9c}$$

$$\psi_4 = \mu e_x = [(v^2 - \mu/r)x - (\boldsymbol{r}^T\boldsymbol{v})u] \tag{9d}$$

$$\psi_5 = \mu e_y = [(v^2 - \mu/r)y - (\boldsymbol{r}^T\boldsymbol{v})v] \tag{9e}$$

Anticipating numerical applications, note that the problem can be nondimensionalized. This aids by making all states roughly the same order. The nondimensionalizations follow:

$$\hat{\boldsymbol{r}} \equiv \frac{\boldsymbol{r}}{r^*} \tag{10a}$$

$$\hat{m} = \frac{m}{m^*} \tag{10b}$$

$$\hat{t} = \frac{t}{\sqrt{r^{*3}/\mu}} \tag{10c}$$

and they require the following:

$$\hat{\boldsymbol{v}} \equiv \frac{\boldsymbol{v}}{\sqrt{\mu/r^*}} \tag{10d}$$

$$\hat{t}_f \equiv \frac{t_f}{\sqrt{r^{*3}/\mu}} \tag{10e}$$

$$\hat{T} \equiv \frac{T/m^*}{\mu/r^{*2}} \tag{10f}$$

$$(\hat{g}_0 \hat{I}_{sp}) \equiv \frac{g_0 I_{sp}}{\sqrt{r^*/\mu}} \tag{10g}$$

The choices of r^* and m^* are completely arbitrary.

Application of Optimal Control

For this problem the choice of performance index is clear:

$$J = m(t_f) \tag{11}$$

where $m(t_f)$ represents the mass of the spacecraft including its fuel at the end of the orbit transfer. The intent, then, is to maximize the performance index, viz., to maximize the mass at the end of the transfer.

The TPBVP is constructed using the necessary conditions in the usual manner.[17] The steering direction vector constraint is included in the Hamiltonian, which can be defined for the optimization problem as

$$H[\boldsymbol{x}(t), T(t), \boldsymbol{e}_T(t), \lambda(t)] = \lambda^T(t)\boldsymbol{f}[\boldsymbol{x}(t), T(t), \boldsymbol{e}_T(t)] + \lambda_e\left[\boldsymbol{e}_T^T(t)\boldsymbol{e}_T(t) - 1\right] \tag{12a}$$

$$H = \lambda_r^T\boldsymbol{v} + \lambda_v^T\left[\left(\frac{T}{m}\right)\boldsymbol{e}_T - \left(\frac{\mu}{r^3}\right)\boldsymbol{r}\right] - \lambda_m\left[\frac{T}{(g_0 I_{sp})}\right] + \lambda_e\left(\boldsymbol{e}_T^T\boldsymbol{e}_T - 1\right) \tag{12b}$$

from which the Euler–Lagrange equations are obtained as ordinary differential equations (ODEs) governing the Lagrange multipliers

$$\dot{\lambda}_r = -\left(\frac{\partial H}{\partial \boldsymbol{r}}\right)^T = \mu\left[\frac{\lambda_v}{r^3} - \frac{3\left(\lambda_v^T\boldsymbol{r}\right)\boldsymbol{r}}{r^5}\right] \tag{13a}$$

$$\dot{\lambda}_v = -\left(\frac{\partial H}{\partial \boldsymbol{v}}\right)^T = -\lambda_r \tag{13b}$$

$$\dot{\lambda}_m = -\left(\frac{\partial H}{\partial m}\right) = \left(\frac{T}{m^2}\right)\lambda_v^T\boldsymbol{e}_T \tag{13c}$$

The next Euler–Lagrange equation is easily derived as

$$\frac{\partial H}{\partial \boldsymbol{e}_T} = \frac{\partial}{\partial \boldsymbol{e}_T}\left[\frac{T}{m}\lambda_v^T\boldsymbol{e}_T + \lambda_e\left(\boldsymbol{e}_T^T\boldsymbol{e}_T - 1\right)\cdots\right] = \frac{T}{m}\lambda_v^T + 2\lambda_e\boldsymbol{e}_T^T = 0 \tag{14}$$

so that the necessary condition is satisfied if $\boldsymbol{e}_T = \lambda_v/|\lambda_v|$ and $\lambda_e = (T|\lambda_v|)/(2m)$; in other words, the thrust direction is parallel to λ_v, which Lawden thus referred to as the pointer vector.[18] This choice is further supported by a sufficient condition. Note that

$$\frac{\partial^2 H}{\partial \boldsymbol{e}_T \partial \boldsymbol{e}_T} = 2\lambda_e\boldsymbol{I} = \frac{T}{m}|\lambda_v|\boldsymbol{I} > 0 \tag{15}$$

when $|\lambda_v| > 0$, $T > 0$, and $m > 0$; if any one of these is violated during a burn, the trajectory is immediately indeterminate.

The switching function is derived by using the maximum principle. The thrust magnitude, which has bounds T_{max} and 0, will give H its maximum value if T is at its maximum value when $H_T > 0$ and at its minimum when $H_T < 0$. The switching function is

$$H_T = \frac{|\lambda_v|}{m} - \frac{\lambda_m}{g_0 I_{sp}} \tag{16}$$

and the switching law is

$$H_T > 0, \qquad T = T_{max}, \qquad H_T < 0, \qquad T = 0 \tag{17}$$

If H_T were to be zero for a finite time period, the control would be singular.

Many authors[13,15,19] have identified the switching law, and associated switching function, as a source of strong sensitivity in numerical solutions.

To complete the TPBVP, optimal control supplies a set of natural boundary conditions

$$\lambda(t_f) = \left\{\frac{\partial G}{\partial \boldsymbol{x}(t_f)}[\boldsymbol{x}(t_0), \boldsymbol{x}(t_f), \nu_0, \nu_f]\right\}^T \tag{18a}$$

$$\lambda(t_0) = -\left\{\frac{\partial G}{\partial \boldsymbol{x}(t_0)}[\boldsymbol{x}(t_0), \boldsymbol{x}(t_f), \nu_0, \nu_f]\right\}^T \tag{18b}$$

where G is defined as

$$G[\boldsymbol{x}(t_0), \boldsymbol{x}(t_f), \nu_0, \nu_f] = m(t_f) + \nu_f^T\{\psi[\boldsymbol{x}(t_f)] - \alpha_f\} + \nu_0^T\{\psi[\boldsymbol{x}(t_0)] - \alpha_0\} \tag{19}$$

and $\psi(\boldsymbol{x})$ was defined in Eqs. (7a–7c) for two dimensions and Eqs. (9a–9e) for three dimensions. Therefore, the natural boundary conditions can be expressed as

$$\begin{bmatrix}\lambda_r(t_f)\\ \lambda_v(t_f)\end{bmatrix} = \left\{\frac{\partial \psi}{\partial \boldsymbol{x}}[\boldsymbol{x}(t_f)]\right\}^T \nu_f \tag{20a}$$

$$\begin{bmatrix}\lambda_r(t_0)\\ \lambda_v(t_0)\end{bmatrix} = -\left\{\frac{\partial \psi}{\partial \boldsymbol{x}}[\boldsymbol{x}(t_0)]\right\}^T \nu_0 \tag{20b}$$

$$\lambda_m(t_f) = 1 \tag{20c}$$

where

$$\left[\frac{\partial \psi}{\partial \boldsymbol{x}}(\boldsymbol{x})\right]^T = \begin{pmatrix}[\boldsymbol{r}_\times] & [2\boldsymbol{r}\boldsymbol{v}^T - (\boldsymbol{r}^T\boldsymbol{v})\boldsymbol{I} - \boldsymbol{v}\boldsymbol{r}^T]^T \\ [-\boldsymbol{v}_\times] & \{(\boldsymbol{v}^T\boldsymbol{v})\boldsymbol{I} - \boldsymbol{v}\boldsymbol{v}^T + \frac{\mu}{(\boldsymbol{r}^T\boldsymbol{r})^{\frac{3}{2}}}[\boldsymbol{r}\boldsymbol{r}^T - (\boldsymbol{r}^T\boldsymbol{r})\boldsymbol{I}]\}\end{pmatrix} \tag{21}$$

and the subscript $\times$ denotes the skew symmetric matrix representation of the cross product.

Finally, for free transfer time the transversality condition must be satisfied:

$$H[\boldsymbol{x}(t_f), \boldsymbol{u}(t_f), \lambda(t_f)] = -\frac{\partial G}{\partial t_f} = 0 \tag{22}$$

New Method for Optimizing Orbit Transfers

The patched method exploits the following idea: any interior one-burn transfer taken between two neighboring coast orbits of an N-burn transfer should be easier to solve than the N-burn transfer as a whole. It then makes sense to consider using the values of the orbital elements of each intermediate coast orbit as free parameters.

Given these parameters (orbital elements, excluding position on orbit), the performance (final mass) is computed by solving each individual one-burn problem in succession. The problem is solved when a local maximum of the final mass is found by varying the free parameters.

The patched method does not enforce satisfaction of Pontryagin's maximum principle. For this problem, Pontryagin's maximum principle supplies the switching law as Eqs. (16) and (17). The method only guarantees that the thrust will switch values at the zeros of the switching function, Eq. (16); it does not guarantee that the polarity will be consistent with Eq. (17). However, this turns out to be an easy condition to check after iterations converge.

A few reasonable and common assumptions are made. It is assumed that the only forces on the spacecraft are spherical-body gravity and the thrust from the rocket motor. The number of arcs of maximum thrust (number of burns) is assumed fixed; choosing the number of burns is often desirable and makes the problem easier to solve. The first and last arcs are assumed to be of maximum thrust; however, under the assumption of spherical-body gravity no generality is lost here. Arcs of intermediate thrust are assumed not to exist in the trajectory because numerical experience indicates that such arcs are rare. It is assumed that no part of the trajectory will

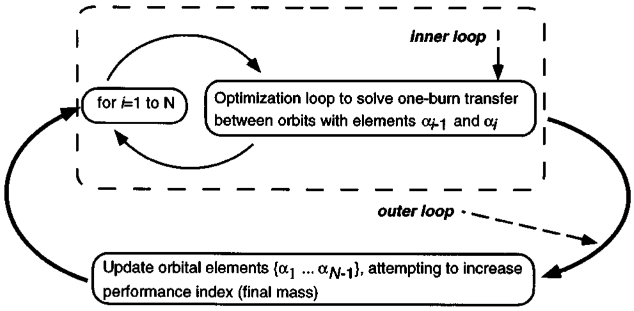

Fig. 1 Diagram depicting the inner-loop and outer-loop structure of the patched method.

be rectilinear; in other words, the angular momentum vector never vanishes. Rectilinear trajectories are unlikely ever to be of interest in an orbit transfer problem, and if they are of interest, the implications of zero angular momentum should motivate the development of specialized methods.

Usually, when a hybrid method is formulated, the assumption is made that the solution to this new problem is always a solution to the original problem. Intuitively, this is often easy to accept. However, it is even more reassuring to be able to show the relationship that exists between the original formulation and what is used by the hybrid method.

What follows shows that necessary conditions from the traditional problem statement are, in fact, equivalent to the necessary conditions that arise from the optimization loop of the patched method. Also, some details of the implemented algorithm are presented.

Architecture of the Method

The architecture of the patched method is best described as an inner and an outer loop. Figure 1 depicts this structure. Given a choice of orbital elements for the terminal orbits of each one-burn subproblem, the inner loop solves each subproblem in succession. Each one-burn transfer has its terminal points and transfer time free for optimization. However, the resulting multiple-burn trajectory is a suboptimal transfer; it lacks the optimal choice of intermediate transfer orbits. The choice of transfer orbits is made by the outer loop via unconstrained minimization of the multiple-burn trajectory's fuel consumption by iterating on the choice of values of the orbital elements for the intermediate transfer orbits.

This approach may be contrasted with multiple-point shooting where some nodes have been forced to coincide with switching times. Such a method combines both the inner and outer loops depicted in Fig. 1. In that case, the whole transfer is determined at one time. For example, if one interrupted a multiple-point shooting algorithm in between iterations, one would find a piecewise-continuous trajectory that may or may not satisfy the boundary conditions. However, if one interrupted the outer loop of the patched method, one would find a continuous trajectory that satisfies the boundary conditions and consists of a sequence of fuel-optimal transfers between fixed orbits (coast arcs). Therefore, as demonstrated later, the Hamiltonian is zeroed on each transfer. If one interrupted the inner loop, then the transfer of the current iteration would be piecewise continuous. The point is not that one of these approaches is better than the other, just that they are different.

The method that has been chosen for the outer loop is the conjugate-gradient method taken from a common reference.[20] Because such a method tends to have better performance if it is supplied with an analytical gradient, such a gradient was formulated for this case; the formulation will be presented in this section.

The architecture of the patched method indicates a useful new paradigm for the orbit transfer problem. That is, one might think of the multiple-burn transfer optimization as the problem of optimizing the fuel used by choosing the intermediate transfer orbits, expressed, given α_0, α_N, m_0, c, and T, as

$$\min_{\alpha_i, i=1,N} \sum_{i=1}^{N} t_{fi}\left[\alpha_{i-1}, \alpha_i, T, c, m_0 - c\sum_{j=1}^{i} t_{f(j-1)}\right] \tag{23}$$

where T is the thrust level, m_0 is the initial spacecraft mass, $t_{f0} = 0$, and $t_{fi}(\alpha_{i-1}, \alpha_i, T, m_i)$ shall be called the transfer time function. The transfer time function computes the optimal transfer time for the orbit transfer problem defined by the initial orbital elements α_{i-1}, the final orbital elements α_i, the thrust level T, the initial mass m, and the fuel consumption rate c. In Eq. (23), the value for the initial mass of each burn is calculated knowing the transfer times for the burns before, giving an unconstrained minimization problem.

In the next section it will be proven that certain conditions necessary to solve Eq. (23) are equivalent to certain conditions necessary to solve the orbit transfer fuel-optimization problem, under certain assumptions. It is not claimed that the two problems themselves are equivalent. It will be seen that the assumptions imposed are few and quite practical.

Computing the Transfer Time Function

Unfortunately, there are no analytical expressions or approximations for the transfer time function. If there were, the separation of this optimization problem would be nicely complete—knowledge of the state and costate time history during a burn would be unnecessary to find the exact multiple-burn extremal transfer. An approximate formulation under certain conditions may be feasible[21]; however, for generality, the patched method computes it numerically in the inner loop. As implemented for this research, the inner loop uses both direct collocation with nonlinear programming (DCNLP)[1] and multiple shooting[19] to solve the one-burn transfer. Each time the optimal solution for a one-burn trajectory is required, either method may be used. For the first iteration, the choice is up to the user. If DCNLP is requested, the solution is found for a high tolerance. Once this tolerance is achieved, a multiple-shooting guess is constructed. Multiple shooting is then used to reduce the error to the desired, lower tolerance. If multiple shooting was requested as the initial method and it fails, a DCNLP guess is constructed, and DCNLP is attempted. If DCNLP is successful, then multiple shooting is used again.

This structure was chosen because it was found that DCNLP was typically much too slow to use with each inner loop iteration but multiple shooting typically could not converge for rough guesses. The failure of multiple shooting typically occurred with the first iteration if the initial guess for the transfer was poor or if the outer loop took too large a step.

At this point, the question of converting the solution from a direct method to a guess for an indirect method arises (the inverse process is trivial because the solution obtained by an indirect method inherently contains more information). Explaining this process requires a look at the adjoined performance index. The adjoined performance index for the jth of N one-burn problems ($j = 1, \ldots, N$) is

$$J_j = m_j(t_j) + \nu_{2j-1}^T\{\psi[\boldsymbol{x}_j(0)] - \alpha_{j-1}\} + \nu_{2j}^T\{\psi[\boldsymbol{x}_j(t_{fj})] - \alpha_j\}$$
$$+ \xi_j^T[m_j(0) - \beta_j] + \int_0^{t_{fj}} \lambda_j^T(t)\{\boldsymbol{f}[\boldsymbol{x}_j(t), \boldsymbol{e}_{Tj}(t)] - \dot{\boldsymbol{x}}_j(t)\}\,\mathrm{d}t \tag{24}$$

where $\boldsymbol{x}_j(t)$ is the state, $u_j(t)$ is the control, t_{fj} is the free final time (the initial time is fixed at 0), α_{j-1} and α_j are the initial and final boundary parameters, $\psi_1(\boldsymbol{x})$ and $\psi_2(\boldsymbol{x})$ are the boundary constraint vector functions, $m_j(t)$ is the spacecraft mass, $\boldsymbol{f}[\boldsymbol{x}_j(t), \boldsymbol{e}_{Tj}(t)]$ is the state dynamics, and $m_j(t_j)$ is the performance index to be maximized. The parameter β_j is fixed while solving each one burn; its value is equal to the initial mass constraint (m_0) or the final mass of the previous burn

$$\beta_j = m_{j-1}\left[t_{f(j-1)}\right] \tag{25}$$

The discretized version for the same problem, divided into M nodes indexed by i and designed for a direct method, follows:

$$\bar{J}_j = \bar{m}_{j,M} + \eta_{2j-1}^T[\zeta_1(\boldsymbol{y}_{j,1}) - \alpha_{j-1}] + \eta_{2j}^T[\zeta_2(\boldsymbol{y}_{j,M}) - \alpha_j]$$
$$+ \sigma_j^T[\bar{m}_{j,i} - \beta_j] + \sum_{i=1}^{M} \mu_{j,i}^T \Delta_i(\boldsymbol{y}_{j,i}, \omega_{j,i}) \tag{26}$$

where $\boldsymbol{y}_i$ is the state, ω_i is the control, $\zeta_1(\boldsymbol{y})$ and $\zeta_2(\boldsymbol{y})$ are the boundary constraint functions, $\Delta_i(\boldsymbol{y}_i, \omega_i)$ are integration constraints, $\bar{m}_{j,i}$

is the spacecraft mass, and $\bar{m}_{j,M}$ is the performance index to be maximized. Assignment of β_j, in this case, is as follows:

$$\beta_j = \bar{m}_{j-1,M} \tag{27}$$

Because, for any $1 < k < M$, both formulations solve the same problem with $j = k$, one can assume that $J_k \approx \bar{J}_k$ for any choice of α_k and α_{k+1} with $\bar{m}_{j-1,M} \approx m_{j-1}[t_{f(j-1)}]$, then

$$\frac{\partial J_j}{\partial \alpha_j} \approx \frac{\partial \bar{J}_j}{\partial \alpha_j}, \qquad \frac{\partial J_j}{\partial \alpha_{j+1}} \approx \frac{\partial \bar{J}_j}{\partial \alpha_{j+1}}$$

$$\frac{\partial J_j}{\partial m_{j-1}[t_{f(j-1)}]} \approx \frac{\partial \bar{J}_j}{\partial \bar{m}_{j-1,M}}$$

One evaluates these partials at the known solutions for both optimal control problems, and the resulting equations are simply

$$\delta J_j = -\nu_{2j-1}^T \delta\alpha_{j-1} - \nu_{2j}^T \delta\alpha_j - \xi_j^T \delta\beta_j \tag{28}$$

$$\delta \bar{J}_j = -\eta_{2j-1}^T \delta\alpha_{j-1} - \eta_{2j}^T \delta\alpha_j - \sigma_j^T \delta\beta_j \tag{29}$$

It is now quite clear that because the gradients were surmised to be approximately equal, then $\nu_{2j-1} \approx \eta_{2j-1}$, $\nu_{2j} \approx \eta_{2j}$, and $\xi_j \approx \sigma_j$.

A simple approach to converting a solution obtained with a direct method into an appropriate guess for an indirect method is now clear. One may use a direct method (DCNLP) to compute η_{2j-1}, η_{2j}, and σ_j; giving values for ν_{2j-1}, ν_{2j}, and ξ_j, then use Eq. (18b) to obtain an approximation of the costates at the initial time. Knowing the states and the costates at the initial time, obtaining an approximate time history merely requires the solution of an initial value problem. This time history can be used as a guess for the indirect method (multiple shooting).

Gradient of the Cost Functional

The cost for the entire transfer is

$$J_f = \sum_{j=1}^{N} t_{fj} = -\frac{g_0 I_{\rm sp}}{T}[m_N(t_{fN}) - m_1(0)] \tag{30}$$

where the mass at the end of the jth burn is a function of α_j, α_{j-1}, and m_{j-1}. This is obviously an equivalent expression to Eq. (23). Omitting some simple steps of calculus and algebra, one may easily write the gradient of the cost functional J_f as

$$\frac{\partial J_f}{\partial \alpha_i} = \frac{-g_0 I_{\rm sp}}{T}\left\{\prod_{j=i+1}^{N-1} \frac{\partial m_{j+1}\left[t_{f(j+1)}\right]}{\partial m_j(t_j)}\right\} \times \left\{\frac{\partial m_{i+1}\left[t_{f(i+1)}\right]}{\partial \alpha_i} - \frac{\partial m_{i+1}\left[t_{f(i+1)}\right]}{\partial m_i(t_{fi})}\frac{\partial m_i(t_{fi})}{\partial \alpha_i}\right\}$$

$$i = 1, \ldots, N-2 \tag{31}$$

$$\frac{\partial J_f}{\partial \alpha_{N-1}} = \frac{-g_0 I_{\rm sp}}{T}\left\{\frac{\partial m_N(t_{fN})}{\partial \alpha_{N-1}} - \frac{\partial m_N(t_{fN})}{\partial m_{N-1}\left[t_{f(N-1)}\right]}\frac{\partial m_{N-1}\left[t_{f(N-1)}\right]}{\partial \alpha_{N-1}}\right\}$$

Equations (31) are not yet sufficient to implement the patched method. Expressions for evaluating the terms in Eqs. (31) are required. To begin, note that m_j is the performance index of the jth burn. Referring back to Eq. (28), one observes that

$$\frac{\partial J_j}{\partial \alpha_{j-1}} = \frac{\partial m_j(t_{fj})}{\partial \alpha_{j-1}} = -\nu_{2j-1}^T \tag{32a}$$

$$\frac{\partial J_j}{\partial \alpha_j} = \frac{\partial m_j(t_{fj})}{\partial \alpha_j} = -\nu_{2j}^T \tag{33b}$$

$$\frac{\partial J_j}{\partial \beta_j} = \frac{\partial m_j(t_{fj})}{\partial m_{j-1}\left[t_{f(j-1)}\right]} = -\xi_j \tag{34c}$$

so that Eqs. (31) can be restated as

$$\frac{\partial J_f}{\partial \alpha_i} = \frac{g_0 I_{\rm sp}}{T}\left[\prod_{j=i+1}^{N-1}(-\xi_{j+1})\right]\left[\nu_{2i+1}^T + \xi_{i+1}\nu_{2i}^T\right]$$

$$i = 1, \ldots, N-2 \tag{35}$$

$$\frac{\partial J_f}{\partial \alpha_{N-1}} = \frac{g_0 I_{\rm sp}}{T}\left[\nu_{2N-1}^T + \xi_N \nu_{2(N-1)}^T\right]$$

This simply gives the gradient of the overall cost function in terms of the Lagrange multipliers from each respective one-burn problem. It is interesting to note that zeroing this gradient supplies simple relations between the Lagrange multipliers associated with the beginning of one burn to those associated with the termination of the previous burn. It is the patching together of optimal burns implied by these relations that inspired the name of the patched method.

Analytic propagation of the costates as implied by zeroing Eq. (35) has been widely studied. The relationship between the costate and state matrizant has provided strong motivation. An early solution was derived by Lawden.[18] Danby[22] has produced a laudable and often noted formulation. The work of Clohessy and Wiltshire,[23] too, has become something of a classic reference. Many other references may be found in Ref. 24, where even another formulation is derived. Other notable and less often referenced works in this area include Refs. 25–27, among others.

Equivalent Set of Necessary Conditions

The following results will prove useful to showing the practicality of the patched method conditions.

Lemma 1: If the matrix $\Gamma \in R^{(n-1)\times n}$ yields rank $(\Gamma) = n-1$ and satisfies $\Gamma \boldsymbol{f} = 0, \boldsymbol{f} \in R^n$ while $\boldsymbol{f}$ satisfies $\lambda^T \boldsymbol{f} = 0, \lambda \in R^n$, and $\boldsymbol{f}^T\boldsymbol{f} \neq 0$, then λ may be expressed as $\lambda = \Gamma^T \nu$ where $\nu \in R^{n-1}$.

Proof: If rank$(\Gamma) = n-1$, $\Gamma\boldsymbol{f} = 0$, and $\boldsymbol{f}^T\boldsymbol{f} \neq 0$, then $\boldsymbol{f}$ is in the null space of Γ, and it is obvious that rank$([\Gamma^T \;\; \boldsymbol{f}]) = n$. This in turn implies that there exists a $\nu \in R^{n-1}$ and $\beta \in R$ such that

$$\lambda = [\Gamma^T \quad \boldsymbol{f}]\begin{bmatrix}\nu \\ \beta\end{bmatrix}$$

Now, $\lambda^T\boldsymbol{f} = 0 \Rightarrow \nu^T\Gamma\boldsymbol{f} + \beta\boldsymbol{f}^T\boldsymbol{f} = 0 \Rightarrow \beta\boldsymbol{f}^T\boldsymbol{f} = 0 \Rightarrow \beta = 0$. □

Lemma 2: Consider the following system of ODEs:

$$\frac{\mathrm{d}}{\mathrm{d}t}\boldsymbol{x}(t) = \boldsymbol{f}(t) \tag{i}$$

$$\frac{\mathrm{d}}{\mathrm{d}t}\lambda(t) = -\left\{\frac{\partial}{\partial \boldsymbol{x}}\boldsymbol{f}[\boldsymbol{x}(t)]\right\}^T \lambda(t) \tag{ii}$$

and a matrix function $\Gamma(\boldsymbol{x})$, if $(\mathrm{d}/\mathrm{d}t)\Gamma[\boldsymbol{x}(t)] + \Gamma(\partial/\partial\boldsymbol{x})\boldsymbol{f}[\boldsymbol{x}(t)] = 0$, then the vector function $\lambda(t) = \Gamma[\boldsymbol{x}(t)]^T\nu$ is a solution to the differential equation (ii).

Proof: To show that a function is a solution to (ii), it suffices to substitute the function into both sides of (ii) and show that equality holds:

$$\text{LHS} = \frac{\mathrm{d}}{\mathrm{d}t}\{\Gamma[\boldsymbol{x}(t)]^T\nu\} = \left\{\frac{\mathrm{d}}{\mathrm{d}t}\Gamma[\boldsymbol{x}(t)]\right\}^T \nu$$

$$\text{RHS} = -\left\{\frac{\partial}{\partial \boldsymbol{x}}\boldsymbol{f}[\boldsymbol{x}(t)]\right\}^T \Gamma[\boldsymbol{x}(t)]^T\nu$$

The left-hand side will equal the right-hand side if $(\mathrm{d}/\mathrm{d}t)\Gamma[\boldsymbol{x}(t)] + \Gamma(\partial/\partial\boldsymbol{x})\boldsymbol{f}[\boldsymbol{x}(t)] = 0$. □

The following definitions are precursors to a theorem that will prove the equivalence between necessary conditions for the patched method, which will be expressed in the definition of conditions {II}, and necessary conditions derived from the usual application of optimal control theory, which will be expressed in the definition of conditions {I}. The specific problem formulation for which such conditions are equivalent will be defined as $\{\boldsymbol{P}\}$.

In what follows, C_i^0 denotes the set of i-dimensional vector functions that are continuous with respect to all arguments, vector and/or scalar, and U denotes the set of piecewise-continuous scalar functions with one scalar argument.

Definition: The optimal control problem $\{\boldsymbol{P}\}$ is of the following form: minimize $J = y(t_f)$ subject to the following constraints:

$$\dot{\boldsymbol{x}}(t) = \boldsymbol{f}[\boldsymbol{x}(t)] + \boldsymbol{g}[y(t), \boldsymbol{v}(t)]u(t), \qquad \boldsymbol{x}(t) \in C_n^0$$

$$\boldsymbol{v}(t) \in C_m^0, \qquad \dot{y}(t) = cu(t), \qquad y(t) \in C_1^0$$

$$0 \le u(t) \le u_{\max}, \qquad u(t) \in U$$

$$\psi[\boldsymbol{x}(t_0)] - \alpha_0 = 0, \qquad \psi[\boldsymbol{x}(t_f)] - \alpha_f = 0$$

$$\psi[\boldsymbol{x}(t)] \in C_{n-1}^0, \qquad y(t_0) = y_0$$

where t_f is free for optimization, t_0 is fixed and satisfying the following assumptions:

1) $\{(\partial\psi/\partial\boldsymbol{x})[\boldsymbol{x}(t)]\}\boldsymbol{f}[\boldsymbol{x}(t)] = 0$
2) $u(t_i) \neq 0$, $u(t_f) \neq 0$, and the number of arcs with $u = u_{\max}$ is N
3) $\boldsymbol{g}[y(t), \boldsymbol{v}(t)]$ is not linear in $\boldsymbol{v}(t)$
4) The solution contains only arcs with $u = 0$ or $u = u_{\max}$
5) $\operatorname{rank}\{(\partial\psi/\partial\boldsymbol{x})[\boldsymbol{x}(t)]\} = n - 1$
6) $\{(\mathrm{d}/\mathrm{d}t)(\partial/\partial\boldsymbol{x})\psi[\boldsymbol{x}(t)] + (\partial/\partial\boldsymbol{x})\psi[\boldsymbol{x}(t)](\partial/\partial\boldsymbol{x})\boldsymbol{f}[\boldsymbol{x}(t)]\} = 0$ when $\dot{\boldsymbol{x}}(t) = \boldsymbol{f}[\boldsymbol{x}(t)]$
7) $\boldsymbol{f}^T[\boldsymbol{x}(t)]\boldsymbol{f}[\boldsymbol{x}(t)] \neq 0 \;\; \forall t \in [t_0, t_f]$

Consider the usual optimal control formulation, introduction of the Lagrange multiplier functions $\hat{\lambda}(t)$, the Hamiltonian $H[\boldsymbol{x}(t), y(t), \boldsymbol{v}(t), u(t), \hat{\lambda}(t)]$ function, and the following partition of $\hat{\lambda}(t)$:

$$\hat{\lambda}(t) = \begin{bmatrix} \hat{\lambda}_x(t) \\ \hat{\lambda}_y(t) \end{bmatrix}, \qquad \hat{\lambda}_x(t) \in C_n^0, \qquad \hat{\lambda}_y(t) \in C_1^0$$

Conditions $\{I\}$*:* For optimal control problem $\{\boldsymbol{P}\}$, the conditions {I} are

$$H[\boldsymbol{x}(t), y(t), \boldsymbol{v}(t), u(t), \hat{\lambda}(t)] = \hat{\lambda}_x^T(t)\boldsymbol{f}[\boldsymbol{x}(t)] + \left\{\hat{\lambda}_x^T(t)\boldsymbol{g}[y(t), \boldsymbol{v}(t)] + c\hat{\lambda}_y(t)\right\}u(t) = 0 \tag{36}$$

$$\frac{\mathrm{d}}{\mathrm{d}t}\hat{\lambda}_x(t) = -\left\{\frac{\partial}{\partial x}\boldsymbol{f}[\boldsymbol{x}(t)]\right\}^T \hat{\lambda}_x(t) \tag{37}$$

$$\frac{\mathrm{d}}{\mathrm{d}t}\hat{\lambda}_y(t) = -\hat{\lambda}_x(t)^T\left\{\frac{\partial}{\partial y}\boldsymbol{g}[y(t), \boldsymbol{v}(t)]\right\}u(t) \tag{38}$$

$$\hat{\lambda}_x(t)^T\left\{\frac{\partial}{\partial \boldsymbol{v}}\boldsymbol{g}[y(t), \boldsymbol{v}(t)]\right\} = 0 \tag{39}$$

$$\hat{\lambda}_x(t_f) = \left\{\frac{\partial\psi}{\partial\boldsymbol{x}}[\boldsymbol{x}(t_f)]\right\}^T \hat{\nu}_f \tag{40}$$

$$\hat{\lambda}_x(t_0) = -\left\{\frac{\partial\psi}{\partial\boldsymbol{x}}[\boldsymbol{x}(t_0)]\right\}^T \hat{\nu}_0 \tag{41}$$

$$\hat{\lambda}_y(t_f) = 1 \tag{42}$$

$$\hat{\lambda}_x(t_{si})^T\boldsymbol{g}[y(t_{si}), \boldsymbol{v}(t_{si})] + c\hat{\lambda}_y(t_{si}) = 0, \qquad i = 1, \ldots, 2(N-1) \tag{43}$$

These are the transversality condition, Eq. (36); the Euler–Lagrange differential equations, Eqs. (37–39); the natural boundary conditions, Eqs. (40–42); and the condition that the switching function vanishes at the switching points, Eq. (43). It is also required by conditions {I} that the control $u(t)$ switch values across each switching point, in a pattern consistent with assumption 2.

Conditions $\{II\}$*:* For optimal control problem $\{\boldsymbol{P}\}$, the conditions {II} are

$$H_i[\boldsymbol{x}(t), y(t), \boldsymbol{v}(t), u(t), \tilde{\lambda}_i(t)] = \tilde{\lambda}_{xi}(t)^T\boldsymbol{f}[\boldsymbol{x}(t)] + \left\{\tilde{\lambda}_{xi}(t)^T\boldsymbol{g}[y(t), \boldsymbol{v}(t)] + c\tilde{\lambda}_{yi}(t)\right\}u(t) = 0 \tag{44}$$

$$\frac{\mathrm{d}}{\mathrm{d}t}\tilde{\lambda}_{xi}(t) = -\left\{\frac{\partial}{\partial\boldsymbol{x}}\boldsymbol{f}[\boldsymbol{x}(t)]\right\}^T \tilde{\lambda}_{xi}(t) \tag{45}$$

$$\frac{\mathrm{d}}{\mathrm{d}t}\tilde{\lambda}_{yi}(t) = -\tilde{\lambda}_{xi}(t)^T\left\{\frac{\partial}{\partial y}\boldsymbol{g}[y(t), \boldsymbol{v}(t)]\right\}u(t) \tag{46}$$

$$u(t) = u_{\max} \tag{47}$$

$$\tilde{\lambda}_{xi}(t)^T\left\{\frac{\partial}{\partial\boldsymbol{v}}\boldsymbol{g}[y(t), \boldsymbol{v}(t)]\right\} = 0 \tag{48}$$

$$\tilde{\lambda}_x(t_i) = -\left\{\frac{\partial\psi}{\partial\boldsymbol{x}}[\boldsymbol{x}(t_i)]\right\}^T \tilde{\nu}_{0i} \tag{49}$$

$$\tilde{\lambda}_x(t_{fi}) = \left\{\frac{\partial\psi}{\partial\boldsymbol{x}}[\boldsymbol{x}(t_{fi})]\right\}^T \tilde{\nu}_{fi} \tag{50}$$

$$\tilde{\lambda}_{yi}(t_{fi}) = 1 \tag{51}$$

$$\tilde{\nu}_{0(i+1)} + \tilde{\lambda}_{y(i+1)}(t_{i+1})\tilde{\nu}_{fi} = 0 \tag{52}$$

$$\left\{\begin{array}{c} \boldsymbol{x}(t_{i+1}) = \boldsymbol{x}(t_{fi}) + \displaystyle\int_{t_{fi}}^{t_{i+1}} \boldsymbol{f}[\boldsymbol{x}(t)]\,\mathrm{d}t \\ y(t) = y(t_{i+1}) = y(t_{fi}) \\ u(t) = 0, t \in [t_{fi}, t_{i+1}] \end{array}\right\} \tag{53}$$

where Eqs. (44–48) are defined for $t \in [t_i, t_{fi}]$, and the following partition is defined

$$\tilde{\lambda}_i(t) = \begin{bmatrix} \tilde{\lambda}_{xi}(t) \\ \tilde{\lambda}_{yi}(t) \end{bmatrix}, \qquad \tilde{\lambda}_{xi}(t) \in C_n^0, \qquad \hat{\lambda}_{yi}(t) \in C_1^0$$

All conditions in {II} are defined for $i = 1, \ldots, N$ except Eqs. (52) and (53), which are defined only for $i = 1, \ldots, N-1$. Finally, $t_1 = t_0$ is assigned and the value for t_f is seen to be t_{fN}.

Theorem 1: If and only if

$$\{\boldsymbol{x}(t), y(t), \boldsymbol{v}(t), u(t), \hat{\lambda}(t) \mid t \in [t_0, t_f]\}, \quad \hat{\nu}_0, \hat{\nu}_f, t_f, \{t_{si} \mid i = 1, \ldots, 2(N-1)\} \tag{54}$$

satisfies {I}, then

$$\{\boldsymbol{x}(t), y(t), \boldsymbol{v}(t), u(t) \mid t \in [t_1, t_{fN}]\}, \quad \{(\tilde{\lambda}_i(t), t \in [t_i, t_{fi}]), t_i, t_{fi}, \tilde{\nu}_{0i}, \tilde{\nu}_{fi} \mid i = 1, \ldots, N\} \tag{55}$$

satisfies {II}, assuming that the constraints and assumptions from $\{\boldsymbol{P}\}$ are satisfied.

Proof: It will be shown, for both the necessary and sufficient parts of the theorem, that if one condition holds, then a construction may be made such that the other is satisfied.

Assume that Eq. (54) satisfies {I}. A solution to {II} will be constructed from Eq. (54) going backward in time. For the last $u = u_{\max}$ arc, where $t \in [t_N, t_{fN}]$, define

$$\tilde{\nu}_{fN} = \hat{\nu}_f \tag{56}$$

$$t_N = t_{s2(N-1)} \tag{57}$$

$$\tilde{\lambda}_N(t) = \hat{\lambda}(t), \qquad t \in [t_N, t_{fN}] \tag{58}$$

These definitions allow Eqs. (36–40) and (42) to imply satisfaction of Eqs. (44–48), (50), and (51) for $t \in [t_N, t_{fN}]$ and $i = N$. Equation (43) for $i = 2(N-1)$ specifies that the switching function is zero at the beginning of this interval, where $t = t_N$. Therefore, satisfaction of Eq. (44) for $i = N$ clearly implies that $\tilde{\lambda}_{xN}^T(t_N)\boldsymbol{f}[\boldsymbol{x}(t_N)] = 0$. Considering this result, Lemma 1, with $\Gamma[\boldsymbol{x}(t_N)] = (\partial\psi/\partial\boldsymbol{x})[\boldsymbol{x}(t_N)]$ and assumptions 1, 5, and 7, implies that there exists a $-\tilde{\nu}_{0N} \in R^{n-1}$ such that Eq. (49) is satisfied for $i = N$. This completes the definitions for the final $u = u_{\max}$ arc.

Consider the next interval, where $t \in [t_{f(N-1)}, t_N]$, the definitions will now be extended into this interval. Define $t_{f(N-1)} = t_{s(2N-3)}$. The conditions {I} specify that $u(t) = 0$ for t in this interval. This implies that Eqs. (53) with $i = N-1$ are consistent with the switching structure of {I}. Define

$$\tilde{\lambda}_{xN}(t) = \hat{\lambda}_x(t), \qquad t \in [t_{fN-1}, t_N]$$

Use of this definition with Eq. (49) satisfied for $i = N$, then Lemma 2, with $\Gamma[\boldsymbol{x}(t)] = (\partial\psi/\partial\boldsymbol{x})[\boldsymbol{x}(t)]$ and assumption 6, implies that the Lagrange multipliers satisfy

$$\tilde{\lambda}_x\left(t_{f(N-1)}\right) = \left\{\frac{\partial\psi}{\partial\boldsymbol{x}}\left[\boldsymbol{x}\left(t_{f(N-1)}\right)\right]\right\}^T[-\tilde{\nu}_{0N}] = \hat{\lambda}_x\left[t_{s(2N-3)}\right]$$

The definition $\tilde{\nu}_{f(N-1)} = -[1/\hat{\lambda}_y(t_N)]\tilde{\nu}_{0N}$ then implies that Eq. (52) for $i = N-1$ is satisfied. The construction for the last $u = 0$ arc is complete.

Define

$$t_{N-1} = t_{s(2N-4)}$$

$$\tilde{\lambda}_{N-1}(t) = \frac{1}{\hat{\lambda}_y(t_N)}\hat{\lambda}(t), \qquad t \in \left[t_{N-1}, t_{f(N-1)}\right]$$

Note that this definition implies satisfaction of Eq. (51) for $i = N-1$ because $\hat{\lambda}_y(t_N) = \hat{\lambda}_y[t_{f(N-1)}]$. This also makes satisfaction of Eq. (52) for $i = N-1$ imply satisfaction of Eq. (50) for $i = N-1$. After establishing these constructions, the arguments for the previous $u = u_{\max}$ and $u = 0$ arc may be repeated. With each repeat, the construction is made with scaling by an even earlier value from $\hat{\lambda}_y(t)$ in the following sequence $\hat{\lambda}_y(t_i), i = N, \ldots, 2$. Such repetition may be continued until the beginning of the first burn is reached. At this point, the definition

$$\tilde{\nu}_{01} = \frac{1}{\hat{\lambda}_y(t_2)}\hat{\nu}_0$$

implies satisfaction of Eq. (49) with $i = 1$ and completes the proof of the if part of the theorem.

Assume that Eq. (55) satisfies {II}. The construction of the solution to {I} will proceed backward in time. Consider the last $u = u_{\max}$ arc, where $t \in [t_N, t_{fN}]$. Define

$$\hat{\nu}_f = \tilde{\nu}_{fN}, \qquad t_{s2(N-1)} = t_N$$

$$\hat{\lambda}(t) = \tilde{\lambda}_N(t), \qquad t \in [t_N, t_{fN}]$$

For $t \in [t_N, t_{fN}]$ and $i = N$, this construction lets Eqs. (44–48), (50), and (51) imply satisfaction of Eqs. (40) and (42) at the final point and Eqs. (36–39) during the interval. Now, it is obvious that satisfaction of Eqs. (36) and (49) with $i = N$ in this interval under assumption 1 implies that Eq. (43) is satisfied for $i = 2(N-1)$; in other words $t_{s2(N-1)}$ is a switching point. This completes the construction for the last $u = u_{\max}$ arc.

The definitions will now be extended into the interval $[t_{f(N-1)}, t_N]$. With Eqs. (53), the conditions {II} specify that $u(t) = 0$ for t in this interval. Define $t_{s(2N-3)} = t_{f(N-1)}$. This implies that Eqs. (53) are consistent with this switching structure of {I} up to and including this interval. Now define

$$\hat{\lambda}_x(t) = \left\{\frac{\partial\psi}{\partial\boldsymbol{x}}[\boldsymbol{x}(t)]\right\}^T[-\tilde{\nu}_{0N}]$$

for all t in this interval. Knowing $u(t) = 0$ and that Eqs. (53) are satisfied in this interval, Lemma 2, with assumption 6 and $\Gamma[\boldsymbol{x}(t)] = (\partial\psi/\partial\boldsymbol{x})[\boldsymbol{x}(t)]$, implies satisfaction of Eq. (37) in this interval is implied. Define

$$\hat{\lambda}_y(t) = \tilde{\lambda}_{yN}(t_N)$$

for all t in this interval. Knowing $u(t) = 0$, this immediately implies satisfaction of Eq. (38) in the interval. Finally, because Eq. (36) was satisfied in the previous interval, Eqs. (37) and (38) are satisfied continuously from $t = t_f$ to any point in the current interval, and because the control switched values at a switching point, then Eq. (36) is satisfied in this interval. This completes the construction for the last $u = 0$ arc.

Define $t_{s(2N-4)} = t_{N-1}$. Consider the interval $[t_{N-1}, t_{f(N-1)}]$. Conditions {II} specify that this is a $u = u_{\max}$ interval, which, by the definitions, is consistent with the switching structure of {I}. Define

$$\hat{\lambda}_x(t) = \tilde{\lambda}_{yN}(t_N)\tilde{\lambda}_{x(N-1)}(t), \qquad \hat{\lambda}_y(t) = \tilde{\lambda}_{yN}(t_N)\tilde{\lambda}_{y(N-1)}(t)$$

in this interval. Equations (44) and (50) with $i = N-1$ imply that $t_{f(N-1)}$ is a switching point. Considering the definitions, Eq. (50) with $i = N-1$ and Eq. (52) with $i = N-2$, obviously continuity of the Lagrange multipliers $\hat{\lambda}_x(t)$ across the switching point $t_{f(N-1)}$ is implied; continuity of $\hat{\lambda}_y(t)$ across this point is immediately implied by the definition. Therefore, Eqs. (37) and (38) are satisfied across the switching point.

The previous arguments for the final $u = u_{\max}$ and $u = 0$ arcs may be repeated, implying satisfaction of the conditions in {I} for each interval. After repeating the arguments and reaching the beginning of the trajectory, the following definitions will have been made and are presented for the sake of clarity:

$$\hat{\lambda}_x(t) = \left[\prod_{j=i+1}^{N}\tilde{\lambda}_{yj}(t_j)\right]\left\{\frac{\partial\psi}{\partial\boldsymbol{x}}[\boldsymbol{x}(t)]\right\}^T[-\tilde{\nu}_{0i}], \qquad t \in \left[t_{f(i-1),t_i}\right]$$

$$i = 2, \ldots, N-1$$

$$\hat{\lambda}_y(t) = \left[\prod_{j=i+1}^{N}\tilde{\lambda}_{yj}(t_j)\right], \qquad t \in \left[t_{f(i-1),\,t_i}\right]$$

$$i = 2, \ldots, N-1$$

$$\hat{\lambda}(t) = \left[\prod_{j=i+1}^{N}\tilde{\lambda}_{yj}(t_j)\right]\tilde{\lambda}_i(t), \qquad t \in [t_i, t_{fi}]$$

$$i = 1, \ldots, N-1$$

Finally, for the first $u = u_{\max}$ interval, one more definition is required. The definition

$$\hat{\nu}_0 = \left[\prod_{i=2}^{N}\lambda_{yi}(t_i)\right]\tilde{\nu}_0$$

forces satisfaction of Eq. (49) with $i = 1$ to imply satisfaction of Eq. (41). □

The theorem does not assure satisfaction of Pontryagin's minimum principle. This principle requires that

$$u(t) = 0 \qquad \text{when} \qquad \hat{\lambda}_x(t)^T\boldsymbol{g}[y(t), \boldsymbol{v}(t)] + c\hat{\lambda}_y(t) > 0$$

$$u(t) = u_{\max} \qquad \text{when} \qquad \hat{\lambda}_x(t)^T\boldsymbol{g}[y(t), \boldsymbol{v}(t)] + c\hat{\lambda}_y(t) < 0 \tag{59}$$

It should be noted that in the application of the patched method to the optimal orbit transfer problem, a second-order condition was taken into account. Lawden's pointer vector theory is a second-order condition and is explicitly specified. Also, note that this condition was determined considering the maximization problem instead of the equivalent minimization problem.

To apply Theorem 1 to the orbit transfer optimization problem, the assumptions of the theorem must be satisfied. Assumptions 1, 3, and 7 are obviously satisfied; however, note that these assumptions require the control to be an angle instead of a unit vector, as in Eq. (4).

There may still be debate over assumption 4; nevertheless, based on numerical experience, orbit transfers that violate assumption 4 are rare if they exist at all.

Assumption 2 is made in anticipation of the ideal gravity assumption. In such a case, coasting before the first burn contributes zero cost and coasting after the final burn contributes zero cost. It therefore makes no sense to allow such arcs as part of the trajectory to be calculated. If an initial and/or final coast arc is desired, it may be added to the computed trajectory without affecting optimality.

Rectilinear orbits will be explicitly excluded from candidate orbit transfer trajectories. Such orbits intersect the center of gravitation and are, therefore, rarely of interest for the orbit transfer problem. With this exclusion made, assumptions 5 and 6 can be shown true for the orbit transfer optimization problem. These exercises are omitted and left for the reader to verify.

Assumption 6 is more than just satisfaction of a simple condition that proves useful to the theorem. In fact, this shows that Eq. (21) is the solution of the ODEs for the Lagrange multipliers, Eqs. (13a–13c), when the Hamiltonian vanishes and ideal gravity is assumed. As reviewed earlier, many previous research efforts have focused on obtaining such solutions.

Solution Using the Patched Method with 11 Burns

The 11-burn solution represented by Fig. 2 represents the current capability of the patched method. For this example, the thrust level is 0.09698, the product $g_0 I_{sp}$ is 0.3929, and the initial mass is 10. The initial orbit is circular with a radius of 1; the final orbit has an eccentricity of 0.398 and a semimajor axis of 1.708. With this information the value of T/W_0 for this transfer is calculated to be 0.009698, placing it at the interface of the low- and medium-thrust transfer ranges.

Figure 2 is a plot of the transfer orbit elements, viz., angular momentum, eccentricity vector x component, and eccentricity vector y component, vs transfer orbit number. The shape of the angular momentum and eccentricity x-component curves seem to indicate a second-order polynomial fit could be used to reduce the number of variables in the problem. The eccentricity y component is always small in this transfer, suggesting that it could be assumed to be zero or, more generally, the same parameterization may be used. The zeroth orbit is the fixed initial orbit, and the eleventh orbit is the fixed final orbit.

Figure 3 shows the angular position of the initial orbit exit point and final orbit entry point of each vs the index enumerating the transfer orbit at which the burn ends. The symmetry of this plot is somewhat surprising. Even though each transfer orbit has its apse roughly aligned with the x axis, each pair of angular positions are not reflected about the x axis. The trend over time is almost exactly opposite between the two positions, but note that the values are not quite the negatives of each other. Also, it is clear that each burn of this transfer is a perigee burn, nearly centered at perigee.

Another interesting trend is found in Fig. 4, showing the burn length vs the same index as before. The burn length decreases monotonically with each successive burn. One can, of course, observe a relationship in the trend of burn length and angular positions from Fig. 3. Both plots have a sharp change at the third burn that, with the fifth burn, returns to follow the trend from the first two. (Note the scale of the vertical axis in Fig. 3—these are not large excursions.) The irregular trend near this burn is attributed to the high tolerance given for the convergence criteria of the outer loop, which chooses the values for orbital elements of the transfer orbits (coast arcs). As this tolerance lowers and the solution becomes more accurate, we expect the trends in Figs. 3 and 4 to appear more linear.

The tolerance for the convergence criteria of the inner loop, on the other hand, was lower. As a result, the Hamiltonian, plotted in Fig. 5 from Eqs. (12b), (16), and (17), evaluated at points equally spaced across each burn, is seen to be quite close to zero with a small variance about zero. This is a reflection of the accuracy with which the inner loop has computed the fuel-optimal one-burn transfer between each prescribed coast arc.

Note that the patched method does not deal directly with values of the states or costates during a coast arc. The outer loop ensures continuity of the costates across coast arcs because optimization of Eq. (30) forces its gradient, Eqs. (35), to vanish. For this solution, the optimality of each burn as a transfer between fixed orbits is more accurate than the optimal choice of transfer orbits (coast arcs), or equivalently, the continuity of the costates along a coast arc. Furthermore, the continuity of the computed solutions to the differential equations (2) and (13a–13c) is the most accurate. This pecking order of accuracy is essential to the operation of numerical analysis software.

The thrust control history for the 11-burn extremal solution is shown in Figs. 6 and 7. Figure 6 shows the control as the angle between the thrust and velocity vectors. This indicates just how close this extremal solution comes to having a tangential thrust control law. Note that the thrust angle never ventures more than 4 deg away from the velocity vector. Furthermore, though the plots show the angle in absolute value, it is clear that each burn has a thrust control law fairly linear in time.

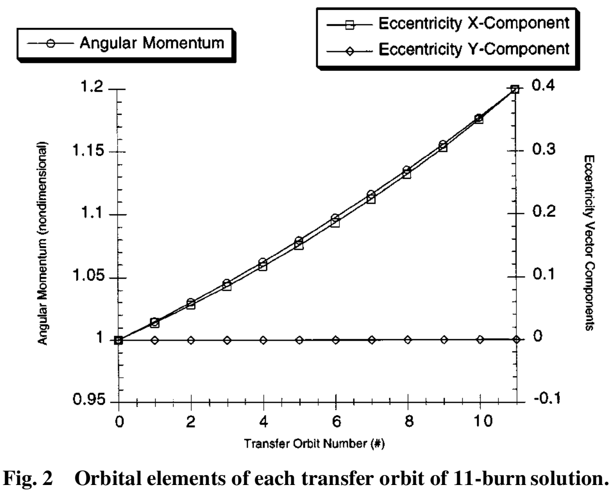

Fig. 2 Orbital elements of each transfer orbit of 11-burn solution.

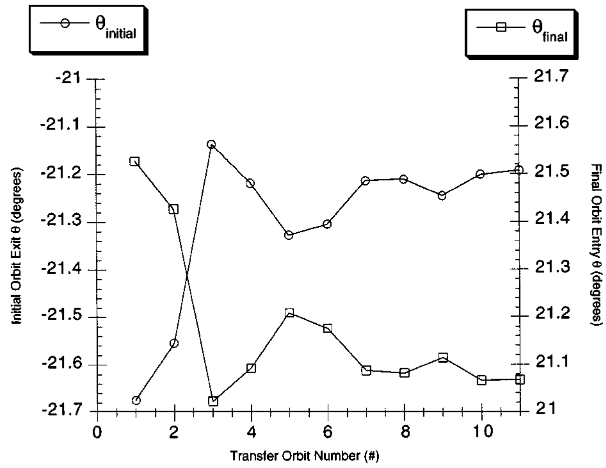

Fig. 3 Orbit transfer terminal points indexed by ending orbit.

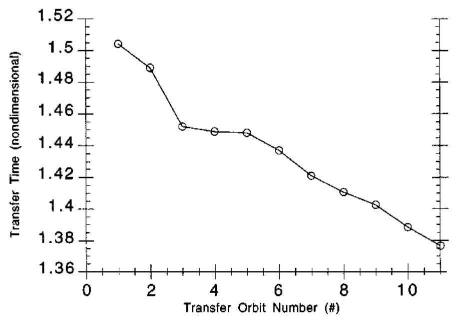

Fig. 4 Transfer time indexed by ending orbit for the 11-burn solution.

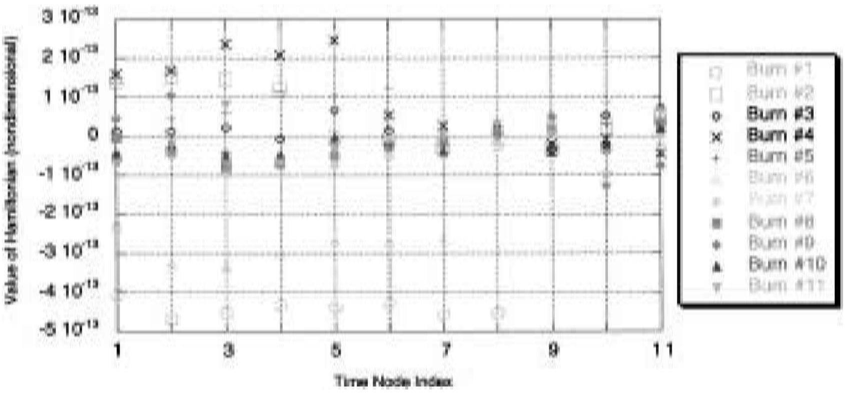

Fig. 5 Hamiltonian along each burn for the 11-burn solution. (Time nodes are spaced evenly throughout each burn.)

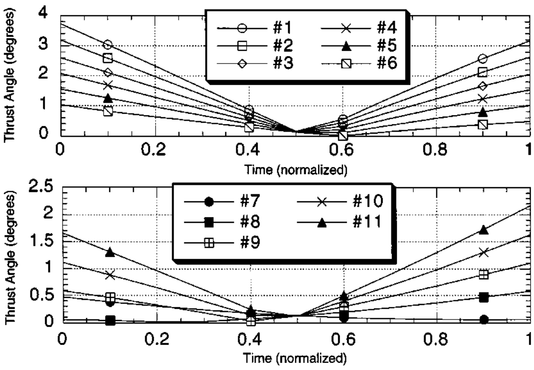

Fig. 6 Angle, in degrees, between the thrust vector and the velocity vector for the 11-burn solution.

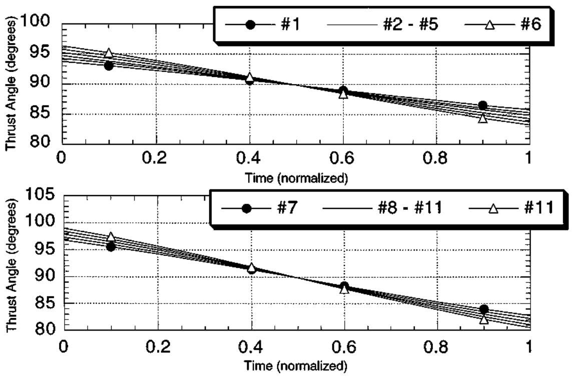

Fig. 7 Angle, in degrees, between the thrust vector and the position vector for the 11-burn solution.

Figure 7 shows the control as the angle between the thrust and position vectors. Shown in this way, the data emphasize the fact that the control has a small, though not likely negligible, radial component throughout the burn. A nearly linear relationship between this angle and time is also apparent.

It should be noted that this solution falls short of having a tangential control law. A reasonable approximation for this control could be a thrust control angle that is measured from the velocity vector and varies linearly with time.

Conclusions

The conditions upon which the patched method is based have been proven equivalent to the optimal control necessary conditions. However, it is required that Pontryagin's maximum principle be checked after iterations have converged.

An interesting spinoff of the theoretical development is a new formulation for the integration of the Lagrange multipliers over a time-optimal coast arc for the nonplanar case assuming ideal gravity. The formulation results from satisfaction of Lemma 2.

Because of its use of a direct method, the patched method was able to obtain the one-burn solutions between each pair of orbits; the multiple-shooting algorithm was not as capable in that aspect. Also, the optimization of the transfer orbits usually proceeded well in the sense that iterations converged. However, the overall method tended to be quite slow because the cumulative time required to compute the one-burn transfers in succession was quite long and increased with the number of burns. Therefore, it is suggested that the patched method be used with a large tolerance to obtain initial results. The result, of course, is inaccurate solutions. On the other hand, these solutions should be good starting guesses for faster, more accurate, yet less robust numerical methods.

Though well suited for a spherical gravity model, the theory developed here does not necessarily extend in a straightforward manner to problems with more complicated gravitational models. In such problems, the orbital elements are not likely constants of integration, and a suitable $\psi(\boldsymbol{x})$ for assumptions 1, 5, and 6 in the preceding theorem becomes difficult to formulate. It may be that, with a complicated gravity model, each burn merely satisfies a rendezvous problem instead of the free-initial/final-points problem. In that case, the patched method may not be so attractive.

The patched method, although not suited for applications requiring rapid computation, has been found to be a fairly robust algorithm for transfers with large numbers of burns. The theory that inspired this method hints at an interesting separation of the optimal transfer problem into several one-burn problems and an unconstrained optimization over the values of the orbital elements. A goal of further research is to develop another method based on this theory where some robustness is traded for much more speed.

Acknowledgment

This research was sponsored by NASA under Contract NAG8-921.

References

[1]Enright, P. J., and Conway, B. A., "Optimal Finite-Thrust Spacecraft Trajectories Using Collocation and Nonlinear Programming," *Journal of Guidance, Control, and Dynamics*, Vol. 14, No. 5, 1991, pp. 981–985.

[2]Hargraves, C. R., and Paris, S. W., "Direct Trajectory Optimization Using Nonlinear Programming and Collocation," *Journal of Guidance, Control, and Dynamics*, Vol. 10, No. 4, 1987, pp. 338–342.

[3]Enright, P. J., and Conway, B. A., "Discrete Approximations to Optimal Trajectories Using Direct Transcription and Nonlinear Programming," *Journal of Guidance, Control, and Dynamics*, Vol. 15, No. 4, 1992, pp. 994–1002.

[4]Betts, J. T., "Optimal Interplanetary Orbit Transfers by Direct Transcription," *Journal of the Astronautical Sciences*, Vol. 42, No. 3, 1994, pp. 247–268.

[5]Coverstone-Caroll, V., and Williams, S. N., "Optimal Low Thrust Trajectories Using Differential Inclusion Concepts," *Journal of the Astronautical Sciences*, Vol. 42, No. 4, 1994, pp. 379–393.

[6]Seywald, H., "Trajectory Optimization Based on Differential Inclusion," *Journal of Guidance, Control, and Ddynamics*, Vol. 17, No. 3, 1994, pp. 480–487.

[7]Vulpetti, G., and Montereali, R. M., "High-Thrust and Low-Thrust Two-Stage LEO-LEO Transfer," *Acta Astronautica*, Vol. 15, No. 12, 1987, pp. 973–979.

[8]Brown, K. R., Harrold, E. F., and Johnson, G. W., "Rapid Optimization of Multiple-Burn Rocket Flights," NASA CR-1430, Sept. 1969.

[9]Brown, K. R., and Johnson, G. W., "Rapid Computation of Optimal Trajectories," *IBM Journal of Research and Development*, Vol. 11, No. 4, 1967, pp. 373–382.

[10]Brusch, R. G., and Vincent, T. L., "Low-Thrust, Minimum-Fuel, Orbital Transfers," *Astronautica Acta*, Vol. 16, No. 4, 1971, pp. 65–73.

[11]McAdoo, S., Jr., Jezewski, D. J., and Dawkins, G. S., "Development of a Method for Optimal Maneuver Analysis of Complex Space Missions," NASA TN D-7882, April 1975.

[12]Kluever, C. A., and Pierson, B. L., "Optimal Low Thrust Earth-Moon Transfers with Switching Function Structure," *Journal of the Astronautical Sciences*, Vol. 42, No. 3, 1994, pp. 269–283.

[13]Redding, D. C., "Optimal Low-Thrust Transfers to Geosynchronous Orbit," NASA Lewis SUDAAR 539, Cleveland, OH, Sept. 1983.

[14]Ilgen, M. R., "A Hybrid Method for Computing Optimal Low-Thrust OTV Trajectories," AAS Rocky Mountain Guidance Conf., AAS Paper 94-129, 1994.

[15]Zondervan, K. P., Wood, L. J., and Caughey, T. K., "Optimal Low-Thrust, Three-Burn Orbit Transfers with Large Plane Changes," *Journal of the Astronautical Sciences*, Vol. 32, No. 3, 1984, pp. 407–427.

[16]Kaplan, M. H., *Modern Spacecraft Dynamics and Control*, Wiley, New York, 1976, pp. 33, 34.

[17]Bryson, A. E., and Ho, Y.-C., *Applied Optimal Control*, Hemisphere, New York, pp. 42–89, 1975, 110–117.

[18]Lawden, D. F., *Optimal Trajectories for Space Navigation*, Butterworths, London, 1963, p. 106.

[19]Chuang, C.-H., Goodson, T. D., and Hanson, J., "Optimal Trajectories of Low- and Medium-Thrust Orbit Transfers with Drag and Oblateness," *Proceedings of the 1994 AIAA Guidance, Navigation, and Control Conference*, AIAA, Washington, DC, 1994, pp. 208–219.

[20]Press, W. H., Flannery, B. P., Teukolsky, S. A., and Vettering, W. T., *Numerical Recipes: The Art of Scientific Computing*, Cambridge Univ. Press, New York, 1989, pp. 301–307.

[21]Alfano, S., and Thorne, J. D., "Circle-to-Circle Constant-Thrust Orbit Raising," *Journal of the Astornautical Sciences*, Vol. 42, No. 1, 1994, pp. 35–45.

[22]Danby, J. M. A., "Matrizant of Keplerian Motion," *AIAA Journal*, Vol. 3, No. 4, 1984, pp. 769, 770.

[23]Clohessy, W. H., and Wiltshire, R. S., "Terminal Guidance System for Satellite Rendezvous," *Journal of Aerospace Sciences*, Vol. 27, No. 9, 1960, pp. 653–658.

[24]Jones, J. B., "A Solution of the Variational Equations for Elliptic Orbits in Rotating Coordinates," *Proceedings of the AIAA/AAS Astrodynamics Conference*, Danvers, MA, Aug. 1980 (AIAA Paper 80-1690).

[25]Glandorf, D. R., "Lagrange Multipliers and the State Transition Matrix for Coasting Arcs," *AIAA Journal*, Vol. 7, No. 2, 1969, pp 363–365.

[26]Vinh, N. X., "Integration of the Primer Vector in a Central Force Field," *Journal of Optimization Theory and Applications*, Vol. 9, No. 1, 1972, pp. 51–58.

[27]Eckenwiler, M. W., "Closed-Form Lagrangian Multipliers for Coast Periods of Optimum Trajectories," *AIAA Journal*, Vol. 3, No. 6, 1965, pp. 1149–1151.